Journal of Machine Engineering, 2022, Vol. 22, No. 2, 108–124
ISSN 1895-7595 (Print)   ISSN 2391-8071 (Online)

Received: *09 February 2022* / Accepted: *22 March 2022* / Published online: *24 March 2022*

cycloid screw surface, five-axis milling machine, ball nose end mill, surface roughness

Van Bong PHAM[1], Nguyen Van THIEN[1]
Van Que NGUYEN[1], Trinh Nguyen DUY[1]
Duy Khanh NGUYEN[1], Dung Hoang TIEN[1*]

PARAMETRIC MODEL ANALYSIS, GEOMETRICAL CHARACTERISTICS AND TOOL TRAJECTORIES TO SURFACE ROUGHNESS WHEN MACHINING THE CYCLOID SCREW BY A FIVE-AXIS MILLING MACHINE

To improve the screw machining accuracy in modern air compressors. This paper investigates three main issues during the development process for cycloid screw machining methods on five-axis CNC machine tools with high precision and efficiency. First, the theoretical basis of cycloid screw surface shaping and derivative of the final profile equation is established. Then, modeling the center trajectory and feed rate according to the cycloid screw profile is given. Next is the experimental setup and simulation of the cycloid screw machining process and discussions. The obtained surface quality prediction parameters are close to the actual measured value, which can be used as a reference model for five-axis CNC milling technology processes. All experimental results obtained by the proposed mathematical model show that a surface with good surface quality is created, meeting the requirements for surface quality. The main work can be used as references for engineers and technicians in practice.

1. INTRODUCTION

Machining components with complex shapes with high precision quickly is a major challenge in machining processes. In particular, the screw of air compressors and oil pumps is one of the typical details for components with complex geometric shapes and high machining accuracy requirements [1, 2]. The screw compressors are powered by two screws, an active screw and a passive screw. During operation, it is necessary to ensure the interaction between the contact surfaces of these screws along spirals with complex curved profiles. When working, the contact helical grooves on the screw change over time, creating cavities that contain gas or liquid, and these liquids or gases are pressed in the axial direction. The geometries of the screws will vary with the number of teeth and the size per shaft, along with the gear ratios and compression ratios with screw sets, however, the contact surfaces between the screws are always the same twisted surfaces with complex profiles. Machining

[1] Faculty of Mechanical Engineering, Hanoi University of Industry, Hanoi city, Vietnam
[*] E-mail: tiendung@haui.edu.vn
https://doi.org/10.36897/jme/147636

of screws is a complex process that always requires specialized tools and equipment [3–5]. These tools and equipment are often expensive, so in this study, the authors focused on the machining of screws on five-axis CNC milling machines and ball nose end mill tools common.

Screw compressors have many advantages such as low vibration and noise along with good dynamic balance, large bearing capacity, small size, less affected by wear during contact and the life of the equipment is long [6, 7]. In air compressors and oil pumps, the screw is the most important component, so the machining process to ensure accuracy and the geometry screw greatly affects the performance of the devices [8, 9]. It can be seen that the screws on air compressors and oil pumps are a special type of gear, with distinctive tooth profiles and twisted surfaces with complex geometries. There are many research and design work on screw profiles, in which the contact lines on the screw surfaces are always the design index of interest in optimizing the screw structure [10, 11]. In general, these screw profile design methods always have technical limitations including the ability to change the shape and geometry size of the screws [12, 13]. Therefore, it is necessary to study more about the theory of shaping screw surfaces for air compressors and oil pumps.

The cycloid screw surfaces are classified into the typical complex surfaces, the machining and manufacturing of these surfaces are difficult to ensure accuracy and surface quality. There have been many studies on the machining methods of twisted surfaces in screw compressors [14, 15]. Studies by Wu et al. [16] have found a definite curve based on the screw characteristics, this curve has been developed which can be used to produce screws with different twisted angles provided that their tooth steps are the same. On this basis, the methods of manufacturing profile cutting tools are mostly used in machining twisted surfaces with the theoretical basis of line meshing [17, 18]. The precision of the twisted movement between the workpiece and the profile cutting tool determines the accuracy of the produced helix surface. With profiling tools, the wear of the cutting tool greatly affects the machining accuracy, in which when the cutting tool has worn the processes of grinding and compensating the cutting tool face many difficulties [19]. These factors lead to very high costs in profiling tool manufacturing as well as screw machining costs. In general, the profiling methods of screw machining are commonly used in mass production.

The cycloid screw has many outstanding advantages over other profile screws and is increasingly widely used in industry, especially in oil pumps, air compressors, gear reducers with high ratio transmission number is large while the size is small [20, 21]. The structure of the cycloid screw is significantly different from that of the general helical screw surfaces [22]. The end face profile of cycloid screw faces is sharper and more similar than other screw faces, that is, there are distinctive lines on the helix surface. In the machining process, the existence of characteristic lines causes difficulty in forming the combined movements between the cutting tool and the workpiece surface, which makes it difficult to manufacture precision profiling cutting tools in cycloid screw surfaces [23]. To overcome this problem, in this study, the authors used standard ball nose milling cutters for cycloid screw machining on a five-axis CNC milling machine. Ball nose end mills have advantages that profile cutting tools do not offer, such as no need to design and build a new cutting tool or machine when machining new shaped parts. The ball nose end mills can be machined with different screw types on standard machining centres, with this feature reducing manufacturing costs.

The technological parameters in the machining process are easily adjusted by the machining centres, thereby finding the optimal machining methods. However, this method also encounters limitations in the machining process such as low machining efficiency with spherical milling cutters, longer machining times compared to profile cutting tools, this process is suitable for producing small batch production with many different screw types. When using the ball nose end mills tool applied to the cycloid screw machining process, the principle of shaping screw surfaces must be studied and analyzed with the geometrical features to be machined.

Based on the above analysis, this paper is designed with the main contents as described below: Theoretical basis of cycloid screw surface shaping and derivative of end profile equation, cycloid curve properties in engineering, cycloid screw profile equation, cycloid screw surface forming process during machining work is presented in Section 2. Parametric modeling of the center trajectory and feed rate according to the cycloid screw profile of the ball nose end mill is given in Section 3. Experimental settings and simulation of cycloid screw machining including collision detection and avoidance in machining, accuracy determination and surface quality after machining are presented in Section 4. The main conclusions of the study are presented in Section 5.

2. THEORETICAL BASIS OF CYCLOID SCREW SURFACE SHAPING AND DERIVATIVE OF THE FINAL PROFILE EQUATION

Compared with other types of screws used in air compressors, compressors using cycloid screws have many outstanding advantages such as high tightness, uniform wear across the entire profile, efficiency high working capacity, large working flow, compact size. Despite such many advantages, manufacturing cycloid screws in air compressors today still face many difficulties due to the requirement to process complex profiles with high precision.

2.1. CYCLOID CURVES USED IN ENGINEERING

The description in Fig. 1 shows that the different Cycloid profiles are generated as the trajectory of a point *M* attached to a circle (C_1) rolling without slipping on another circle (C_2). Depending on the position of the point *M* relative to the rolling circle (C_2), it can be divided into three different types of cycloid curves: the first case, if the point *M* lies on (C_1), it will create a cycloid; the second case, the point *M* lies in (C_1), will create a contraction cycloid; the third case, if the point *M* is outside (C_1), will create an extensor cycloid. Based on the relative positions between the two circles (C_1) and (C_2), the cycloids can be divided into two types, Epi-cycloid and Hypo- cycloid. If two circles (C_1) and (C_2) lie outside each other, the resulting cycloid is called an Epi-cycloid as shown in Fig. 1a. If two circles (C_1) and (C_2) lie in each other, the resulting cycloid is called a Hypo-cycloid as shown in Fig. 1b. In the case of a circle with radius (C_2) of infinity, this process forms a cycloid as depicted in Fig. 1c.

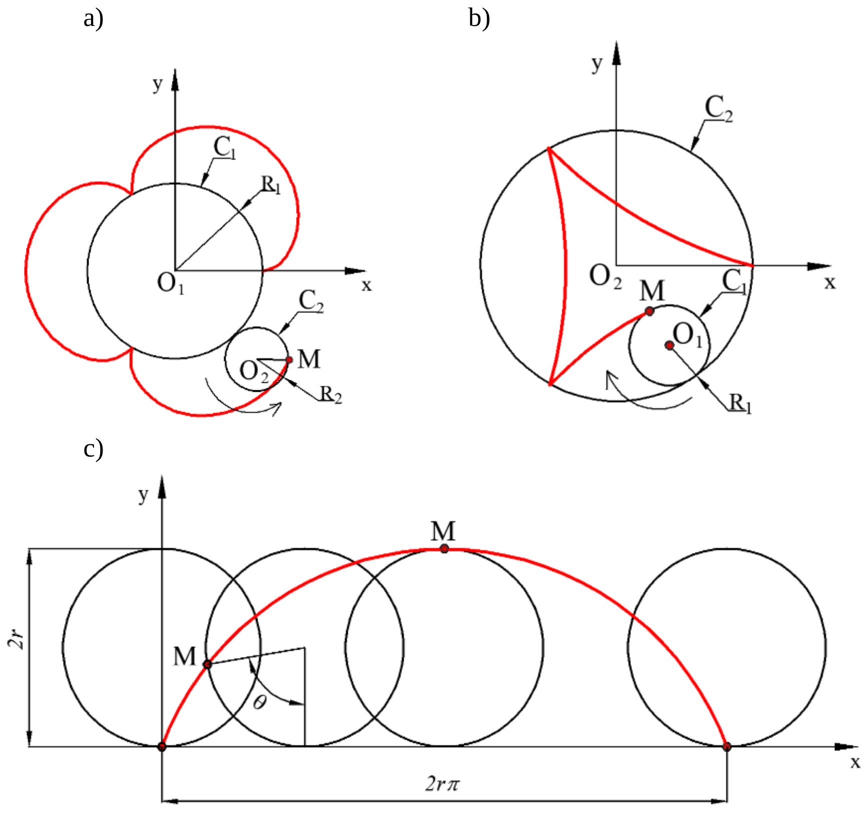

Fig. 1. Principle of shaping cycloid curves: a) Epi-cycloid, b) Hypo-cycloid, c) Cycloid

2.2. CYCLOID SCREW PROFILE EQUATION

The mathematical expression of the cycloid screw tooth profile is established according to the surface shaping principle. According to the meshing principle of the screw teeth during the engagement of two screws with the same mesh size. When a pair of screws engages during work, the upper teeth of one screw will match the lower curve of the other screw. As shown in Fig. 2, the tooth face of the screw includes the *BC* segment, followed by the anterior and dorsal face of the tooth with a cycloid profile (*AB* and *CD*), the exit groove includes the *DEG* arc.

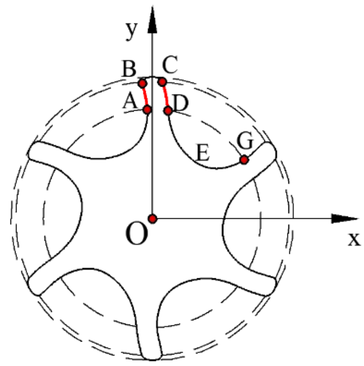

Fig. 2. The cycloid screw profile

According to the shaping principle, the cycloid profile equation of the screw tooth is shown by the following equation [22]:

$$\begin{cases} x = r_b \times (\cos\theta + \theta \times \sin\theta) \\ y = r_b \times (\sin\theta - \theta \times \cos\theta) \end{cases} \tag{1}$$

where r_b is the radius of the base circle, *x* and *y* are the cycloid screw coordinates, and θ is the cycloid opening angle. Figure 3 depicts the process of forming a cycloid screw profile, when step circle *B* of one screw tooth rolls without sliding on the pitch circle *A* of the other screw, the point T_1 is the point of the auxiliary circle where the ring is located step circle *B*, the curve trajectory created by point T_1 is the curve intersecting the step circle *A*. The distance between the T_1 point and the T_2 non-slip rolling point with centre O_1 is constant during the meshing.

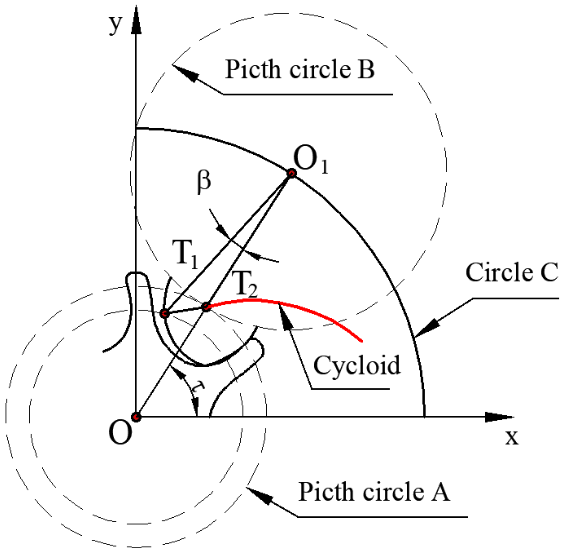

Fig. 3. The cycloid screw profiles process forming

With $r_a = T_1O_1;\ \beta = T_1O_1T_2;\ r_p = T_2O_2$ then T_1T_2 is determined by

$$T_1T_2 = h = \sqrt{r_p^2 + r_a^2 - 2 \times r_p \times r_a \times \cos\beta} \tag{2}$$

where r_p is the radius of the orbit of the coordinate center O_1 of the circle *C* with coordinates:

$$\begin{cases} x_1 = 2 \times r_p \times \cos\tau \\ y_1 = 2 \times r_p \times \sin\tau \end{cases} \tag{3}$$

The trajectory of the motion of point T_2 is a cycloid defined by the following equation:

$$\begin{cases} x_2 = 2\times r_p \times\left[\cos\tau - \dfrac{1}{2}\cos\left(2\tau - \dfrac{\pi}{4}\right)\right] \\ y_2 = 2\times r_p \times\left[\sin\tau - \dfrac{1}{2}\sin\left(2\tau - \dfrac{\pi}{4}\right)\right] \end{cases} \tag{4}$$

where τ is the angle established between the x-axis and OO_1.The curve equation of the arc DEG is determined by:

$$\begin{cases} r_a^2 = \left(x - x_1\right)^2 + \left(y - y_1\right)^2 \\ h^2 = \left(x - x_2\right)^2 + \left(y - y_2\right)^2 \end{cases} \tag{5}$$

From equation (5) with parameters x_1, y_1, x_2, y_2 defined in formulas (3) and (4), the parametric equation of the DEG segment is obtained.

Through the geometric analysis of the screw tooth profile, the mathematical expression of the screw tooth surface will be determined, which lays the mathematical foundation for the parametric model in 3D machining of the screw profile.

2.3. THE PROCESS OF FORMING A CYCLOID SCREW SURFACE DURING MACHINING

Figure 4 depicts a coordinate system that deals with $Oxyz$ with $\vec{i}, \vec{j}, \vec{k}$ being the unit vectors of the three respective coordinate axes. Then the vector of the cycloid curve R in space is described by the equation:

$$R_O = R_O\left(u\right) \tag{6}$$

When the cycloid curve has a torsional motion to form a screw tooth profile, the cycloid screw surface is generated then the R curve has two motions, one rotation around the z-axis and one translational motion along the z-axis, The grooved orbital surface is created by the cycloid R curve in space is a cylindrical surface with the $z(k)$ axis.

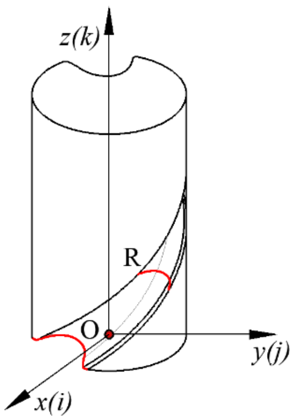

Fig. 4. Principle of shaping screw surface with a cycloid profile

2.4. ESTABLISH THE CYCLOID SCREW SURFACE EQUATION

The cycloid equation in the first quadrant *xOy* plane of the *Oxyz* coordinate system is represented by the following equation [24]:

$$\begin{cases} x(\phi) = r_\phi \times \left[\phi \times \sin(\phi+\beta) + \cos(\phi+\beta)\right] \\ y(\phi) = r_\beta \times \left[\phi \times \cos(\phi+\beta) + \sin(\phi+\beta)\right] \end{cases} \tag{7}$$

where r_β: base radius invariant, ϕ: rolling angle of the point invariant with $\phi \in [\phi_1, \phi_2]$, β: rotation of the invariant starting point on the base circle. The twisted surface is formed as shown in Fig. 5 with the invariant curve $r_\beta = r(u)$ torsion around the z-axis with the helical parameter $p = \frac{\pi}{2}$.

The screw surface equation is determined by:

$$S(\theta,\phi) = \begin{cases} r_\phi \times \left[\phi \times \sin(\phi+\beta+\theta) + \cos(\phi+\beta+\theta)\right] \\ r_\beta \times \left[\phi \times \sin(\phi+\beta+\theta) + \cos(\phi+\beta+\theta)\right] \\ p \times \theta \end{cases} \tag{8}$$

where θ is the rotation angle of the invariant curve *r(u)* around the z-axis.

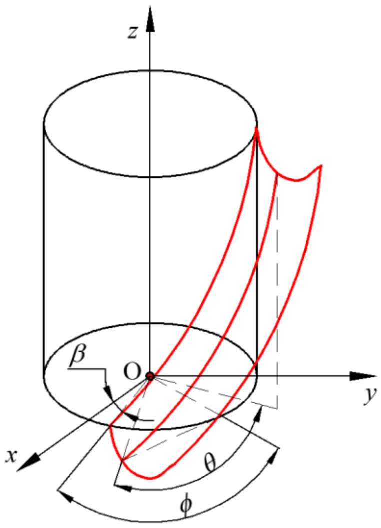

Fig. 5 The screw surface forming process

During machining by five-axis CNC machining centres, the process of determining the normal vector on the surface is very important in calculating the tool center coordinates. If β in the invariant screw surface equation is a constant, with $S = \sqrt{r_\beta^2 + p^2}$ then the unit normal vector of the surface can be expressed as

$$n_O = \frac{\left(\frac{\partial S}{\partial \phi} \times \frac{\partial S}{\partial \theta}\right)}{\left|\frac{\partial S}{\partial \phi} \times \frac{\partial S}{\partial \theta}\right|} = \left[\frac{p \times \sin(\phi + \beta + \theta)}{S}, -\frac{p \times \cos(\phi + \beta + \theta)}{S}, \frac{S_\beta}{S}\right] \tag{9}$$

The coordinate of the tool center relative to the working point is the coordinate value of the unit normal vector of the tip and the radius of the tool. With *R* being the spherical tool radius, then the tool center coordinates are determined by

$$\begin{cases} x = \dfrac{r_\beta \times \left[\phi \times \sin(\phi + \beta) + \cos(\phi + \beta) + p \times R \times \sin(\phi + \beta)\right]}{S} \\ y = \dfrac{r_\beta \times \left[-\phi \times \cos(\phi + \beta) + \sin(\phi + \beta) - p \times R \times \cos(\phi + \beta)\right]}{S} \\ z = \dfrac{r_\beta \times R}{S} \end{cases} \tag{10}$$

The distance between the center of the cutting tool and the constant screw surface is determined by:

$$\left[\frac{R \times p \times \sin(\beta + \phi)}{S}, -\frac{R \times p \times \cos(\beta + \phi)}{S}, \frac{r_\beta \times R}{S}\right] \tag{11}$$

With the z-direction constant, the sum of squares of the x and y vector coordinates between the cutter center and the cycloid screw surface is determined by the following formula:

$$\frac{p^2 \times R^2}{S^2} = \left(-\frac{R \times p \times \cos(\beta + \phi)}{S}\right)^2 + \left(\frac{R \times p \times \sin(\beta + \phi)}{S}\right)^2 \tag{12}$$

This result shows that the vector distance between the tool center and the torsion surface is constant as a constant $\frac{r_\beta \times R}{S}$ in the direction parallel to the z-axis. With the screw end profile known then the machining position of the tool center in the z-axis direction can be obtained by displacements of the distance $\frac{r_\beta \times R}{S}$ in the z-direction. Based on the unique geometric properties of the screw surface the mathematical bases for screw machining with standard ball nose end milling cutters are established.

3. MODELING THE CENTER TRAJECTORY AND FEED RATE ACCORDING TO THE CYCLOID SCREW PROFILE

In this study standard ball nose milling cutters were used for machining cycloid screws on a five-axis CNC milling machining centre. The milling process is depicted as shown in

Fig. 6 with the finished profile curve of the screw formed by interpolating motion of the *y* and *z*-axes, interpolating the *x*-axis and the *A*-axis driving the screw to produce torsional motion, the two axes interact with the interpolated motion of the five-axis machine tool used to mill the cycloid screw surfaces. The relationship between screw rotation speed and feed rate during machining is depicted in Fig. 6, the screw reciprocating motion in the *x*-axis direction and at the same time rotating around the *x*-axis, the machine feed rate five-axis milling is concerned with the rotational speed and size of the screw. Given the rotational speed of the workpiece of the screw is ω and its pitch is l, then the feed rate is $f = \frac{l \times \omega}{2\pi}$.

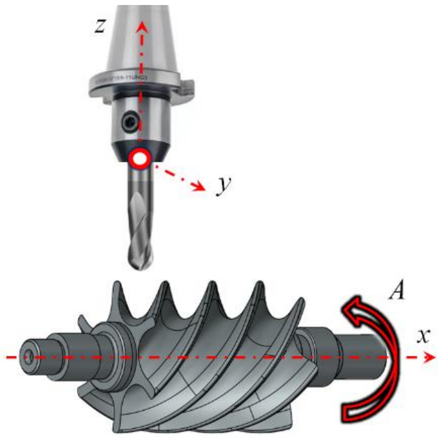

Fig. 6. The cycloid screw milling mechanism on a five-axis milling machine

3.1. THE CYCLOID SCREW MILLING MODEL

The cycloid profile curves of the screw are designed by NX software. After the profile curves are generated, the end profile of the screw is generated as shown in Fig. 7a. Then the end profile is considered as the sweep, the screw is the initial trajectory curve, the helix on the corner circle is as a cycloid orbital curve to scan along the helix and obtain the tooth profile of the screw. Finally, the 3D model of the cycloid screw was obtained using the generated tooth as shown in Fig. 7b. Where the screw cycloid model is a parametric module, that is, a new 3D screw model can be created in the NX software by changing the basic parameters of the screw.

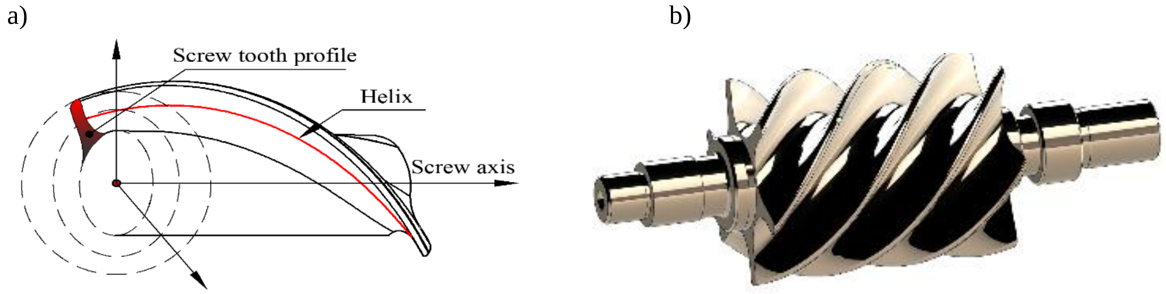

Fig. 7. The cycloid tooth profile and 3D screw model: a) the cycloid tooth profile, b) 3D model of cycloid screw

3.2. THE CENTER ORBIT OF BALL NOSE END MILLS TOOL IN CYCLOID SCREW MACHINING

The tool trajectory profile is interpolated from the cycloid profile, so the distance between the tool center and the helix surface is a constant in the *xOy* plane. The description in Fig. 8 shows the coordinates of the calculation of the interpolation point P, then the coordinates of the center *P** are determined by:

$$L_{OP}^{*} = L_{OP} + PP^{*} = L_{OP} + \frac{dn}{|n|} \tag{13}$$

where *d* constant n: normal vector of point *P* on the screw surface.

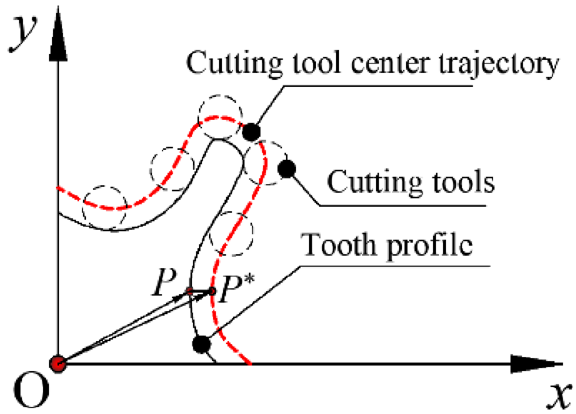

Fig. 8. Model for determining the cutting tool center trajectory

4. EXPERIMENTAL SETUP AND SIMULATION OF THE CYCLOID SCREW MACHINING PROCESS

Figure 9 depicts the test procedure for cycloid screw machining. From the 3D cycloid screw design model, the machining programming processes are simulated and performed with NX software, when the software simulation process is thoroughly tested, the program will be output NC for the machining process.

Initially, the machine and the programming coordinate system are set up to give the motion relationship of the tool relative to the workpiece surface. The right machining parameters are established for the five-axis milling simulation based on the precision machine tool and machine system. If the NC program is output from the NX software, no errors or abnormal problems arise, the machining process is performed. After the experimental processes, the roughness measurement process was performed to check the quality of the machined surface, thereby seeing the feasibility and meeting the needs of the proposed machining model. The image simulates the five-axis milling process by NX software as shown in Fig. 10.

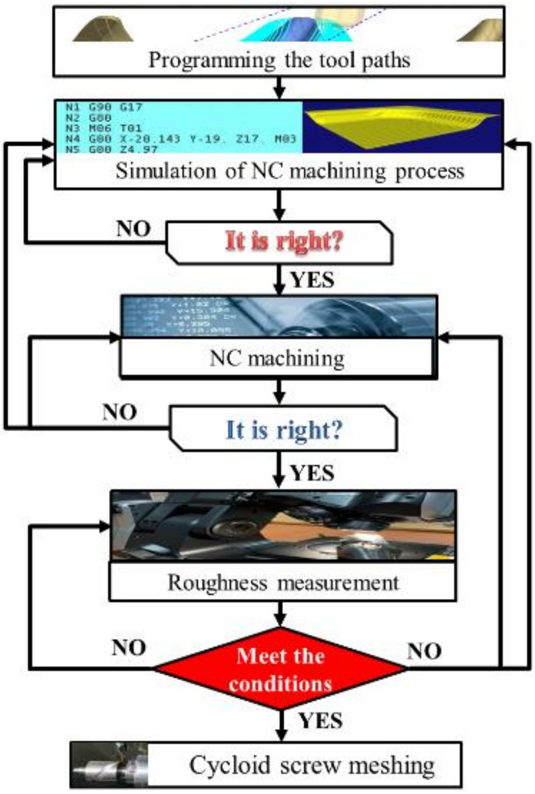

Fig. 9. Diagram of experimental design for cycloid screw machining

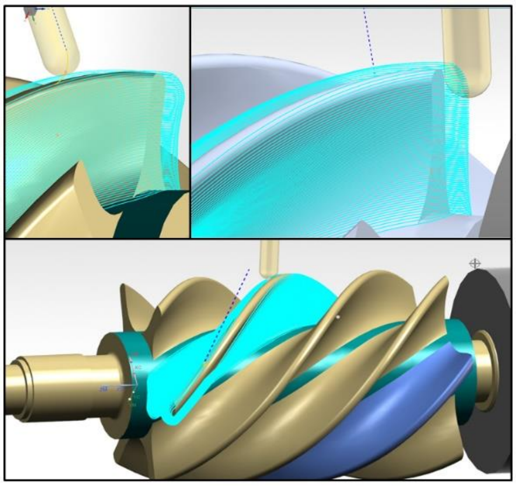

Fig. 10. Image simulation of cycloid screw machining process

4.1. COLLISION DETECTION AND AVOIDANCE IN CYCLOID SCREW MACHINING

The machine tool feed system is located on the A-axis, the machine tool machining program is controlled by the machine tool main axis with the interpolated movement of the *y*-axis and the *z*-axis with the NC code of the *x*-axes and axis *A* as shown in Fig. 11.

The NC programs show that, during *z*-axis machining at a safe feedback height, before machining, the *z*-axis goes down, and the *y* and *z*-axis perform interpolated movements to complete the machining process. At the end of the machining processes the *A*-axis and the *x*-axis return to zero with which the *z*-axis is returned to the required safe height. This process helps the machining method avoid collisions between the cutting tool and the workpiece. In addition, the authors choose the radius of the spherical milling cutter according to the minimum radius of curvature of the screw end face curve, this process enables the ability to effectively remove the workpiece residue while ensuring conformance to the curved profile of the screw surface at different machining positions.

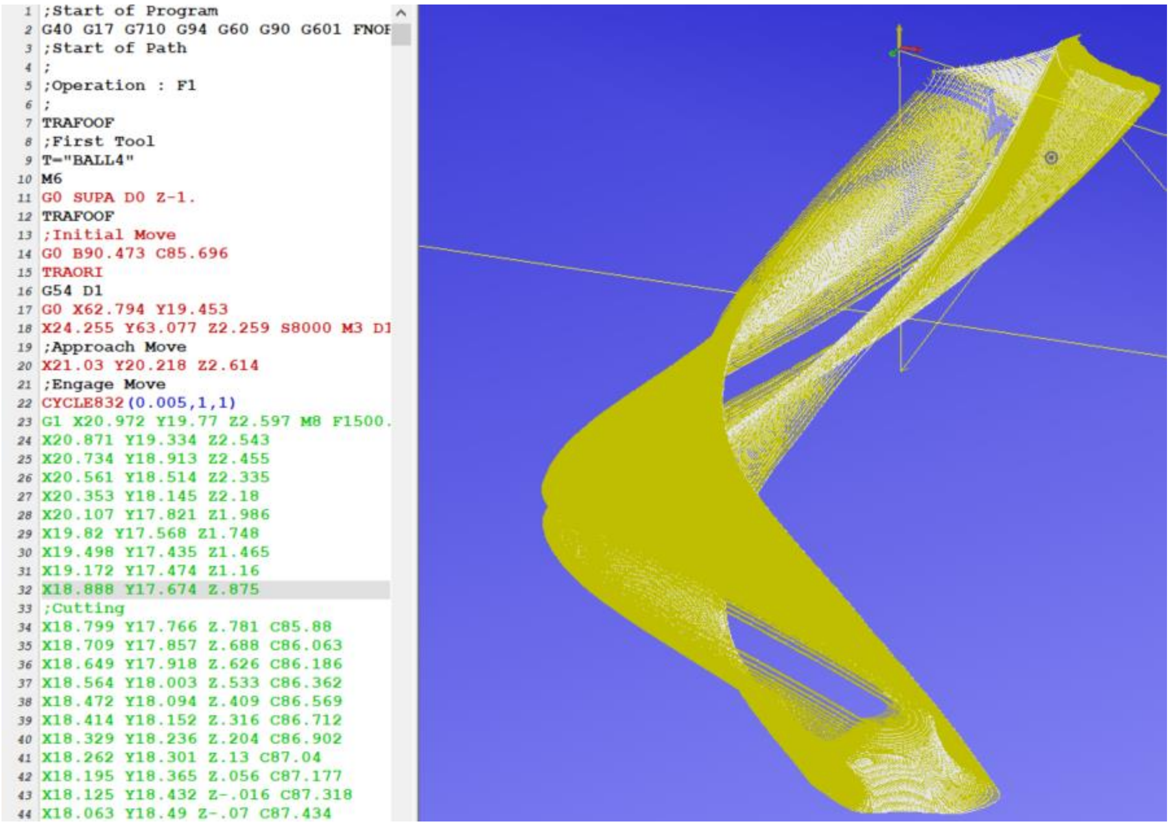

Fig. 11. NC program for machining cycloid screw tooth profiles

4.2. THE CYCLOID SCREW MACHINING EXPERIMENT

The DMU-50 Mori five-axis CNC milling machine is used in cycloid screw machining. System of experimental equipment in screw machining using HSLB-2030 ball nose end mills as shown in Fig. 12. The design parameters of the cycloid screw are shown in Table 1. The vibration measuring device includes accelerometer 4525-B-001 acquired by a data processor and PLUSE software. The material used in the cycloid screw machining experiments is 40Cr steel. This is a commonly used material in parts subject to heavy loads. The chemical composition of 40Cr steel is described in Table 2.

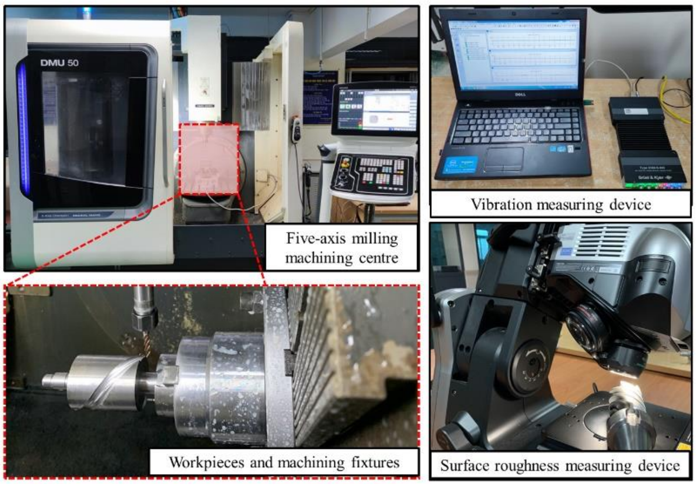

Fig. 12. Image of cycloid screw processing equipment

Table 1. Technological parameters of cycloid screw

Tooth profile	Number of flutes	Twisted angle	Module	Pressure angle	Screw section length
Cycloid	6	32°	15	20°	65 mm

Table 2. Composition of elements in 40Cr steel

Grade	Chemical composition (% weight)						
	C	Mn	Si	Cr	Ni	P	S
40Cr	0.37~ 0.44	0.50 ~ 0.80	0.17 ~ 0.37	0.80 ~ 1.10	≤0.030	≤0.035	≤0.035

4.3. PRECISION AND SURFACE QUALITY OF CYCLOID SCREW MACHINED

Machining accuracy is assessed through the machined surface and the original design surface must match. In this work, the accuracy and surface roughness determined through the average surface roughness Ra and meshing of the cycloid screw are combined to determine if the developed model meets the requirements. Roughness tests were performed on a Keyence VHX-7000 roughness measuring instrument with the measured data used for comparison with the predicted values of Ra.

Surface roughness prediction during five-axis CNC milling is an experimental problem. This approach aims to meet the increasingly exacting and rigorous technological requirements. The implementation of a specific material and technology system is extended to the same types of classes. The experiments were carried out under different cutting conditions and in triplicate in which two initial data sets were used in the training processes, and the third set of experiments was performed to predict the surface roughness. The technological parameters that were changed during the experiment are shown in Table 3.

The analysis and experiment results are compared to confirm the accuracy of the proposed model. In this work, the approach of applying the back-propagation neural network and multi-objective particle swarm optimization (BPNN-MOPSO) hybrid algorithm to help provide the ability to predict the surface quality that we have given in the previous work [25], has the ability to predict with high accuracy. After the experimental procedures, the surface roughness was measured at different positions on the cycloid surface on the helix groove. Figures 13 and 14 show the surface roughness prediction in Ra based on the front and back teeth under different machining conditions.

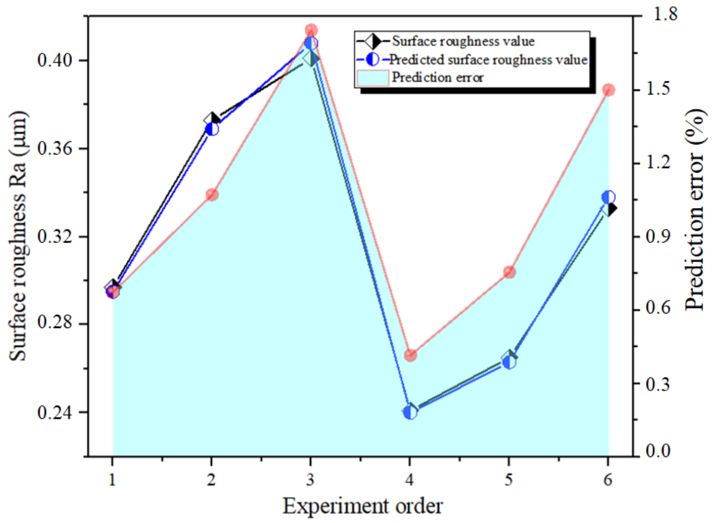

Fig. 13. Predicted and measured surface roughness on the front face of the screw tooth

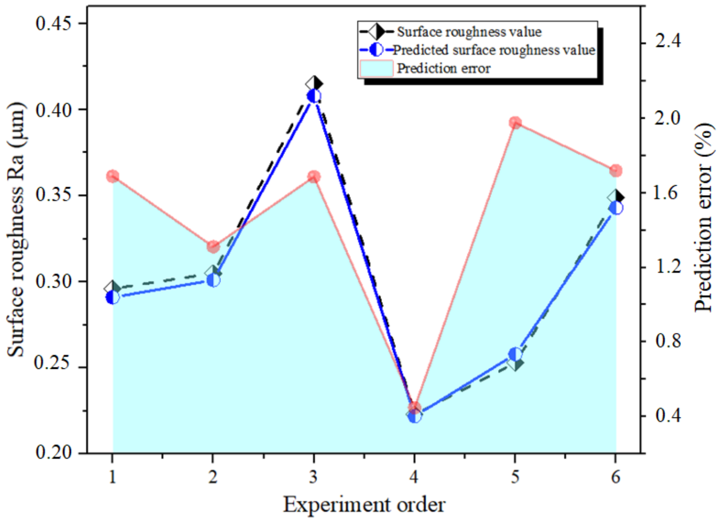

Fig. 14. Predicted and measured surface roughness on the back face of the screw tooth

The surface roughness measurement results in Table 3 show that when increasing the cutting speed the surface quality increases while increasing the feed rate the surface quality decreases. Besides, the relationship between vibration amplitude and surface quality is also seen, when at the same cutting speed, the vibration amplitude increases, indicating a decrease in surface quality. The surface finish obtained after machining on the anterior and dorsal surfaces of the cycloid screw is not significantly different, indicating stability on all machining surfaces. The obtained surface quality prediction parameters are close to the actual measured value, which can be used as a reference model for five-axis CNC milling technology processes.

The image of the screw after machining is shown in Fig. 15, from the images and experimental results show that the cycloid screw machined by the mathematical model completely meets the accuracy requirements. The obtained results show the correctness of the mathematical expression and model for cycloid screw machining on a five-axis CNC machining center by a ball nose end mill tool.

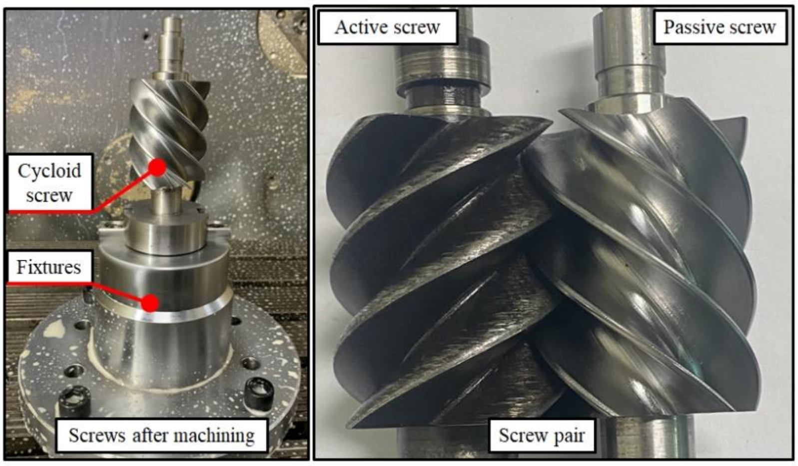

Fig. 15. Image of the cycloid screw after machining

Table 3. Parameters and experimental results of cycloid screw machining

No.	Spindle speed n (rpm)	Cutting speed Vc (m/min)	Depth per Cut (mm)	Feed rate f (mm/min)	Vibration amplitudea (m/s^2)	Front surface roughness Ra (μm)	Dorsal surface roughness Ra (μm)
1	8000	100	0.002	1300	9.637	0.297	0.296
2	8000	100	0.004	1300	10.935	0.373	0.305
3	8000	100	0.006	1300	13.993	0.401	0.415
4	11000	140	0.002	1800	7.188	0.241	0.223
5	11000	140	0.004	1800	10.738	0.265	0.253
6	11000	140	0.006	1800	12.794	0.333	0.349

5. CONCLUSION

In this work, the screw cycloid profile equations are given. From the cycloid profile equation and the formation principle of the helical surface, the parametric model of the cycloid screw was established. This study proposes a method for machining the cycloid screw according to the properties of the torsion surface with a standard ball nose end mill tool.

Simulations of machining processes and experiments performed by NC programs along with surface quality measurement parameters show that the research method fully meets the requirements for accuracy as well as the quality of the cycloid screw. Compared with the previous cycloid screw profile design method, the proposed model is set up as a parameter, with a 3D model of the screw that can be created by changing screw parameters right in the software, the screw design and machining process is more flexible, convenient and accurate.

Compared with the method of machining by profile cutting tools, the proposed method based on ball nose end milling cutters has the following advantages: The cutting tool is a standard milling cutter so the machinability as well as easier to change cutting tools. Easily compensate tool length and radius in CNC machining processes. Easily set up dynamic simulation processes of the machining process through which cutting tool collisions are detected, and technology parameters are easily adjusted to create screws with better surface quality.

The surface quality results obtained show that the cycloid screw machined by the mathematical model completely meets the accuracy requirements. The surface roughness obtained after machining on the front and back surfaces of the cycloid screw is not significantly different, indicating stability on all machining surfaces. The obtained results show the correctness of the mathematical expression and model for cycloid screw machining on a five-axis CNC machining center by a ball nose end mill tool.

The general mathematical model for machining cycloid screws by ball nose end mills established in this study can be useful for screw manufacturers or CNC machine developers to simulate machining motions and evaluate the machining result of the screw. Through the method applied in this study, it can also be used to process some other complex surfaces.

In future studies based on the postprocessing technology, the basic kinematic model of the five-axis machine tool combined with the angle optimization algorithm and stochastic tool wear to solve the problem of machining cycloid screws and improve the processing efficiency.

REFERENCES

[1] BIZZARRI M., BARTON., 2021, *Manufacturing of Screw Rotors Via 5-axis Double-Flank CNC Machining*, Computer-Aided Design, 132, 102960, https://doi.org/10.1016/j.cad.2020.102960.

[2] WU Y.-R., HSU W.-H., 2014, *A General Mathematical Model for Continuous Generating Machining of Screw Rotors with Worm-Shaped Tools*, Applied Mathematical Modelling, 38/1, 28–37, https://doi.org/10.1016/j.apm.2013.05.056.

[3] HERAN Y., XINGWEI S., FEI P., TONGCHUN Y., 2017, *Contact Analysis for the Process of Dual Abrasive Belt Polishing Screw Curved Surface*, Procedia Computer Science, 107, 743–748.

[4] WANG S., WANG Z., SHI H., WANG Z., HAO M., WANG J., 2021, *Study on Screw Rotor Thermal Machining Method of Single Screw Compressor*, IOP Conference Series: Materials Science and Engineering, 1180, 012011.

[5] WANG C., WANG B., LIU M., XING Z., 2022, *A Review of Recent Research and Application Progress in Screw Machines*, Machines, 10/1, https://doi.org/10.3390/machines10010062.

[6] BASHA N., KOVACEVIC A., RANE S., 2021, *Numerical Investigation of Oil Injection in Screw Compressors*, Applied Thermal Engineering, 193/5, 116959, https://doi.org/10.1016/j.applthermaleng.

[7] WANG Z,. XING., SUN S., YU Z.C., 2021, *Development and Experimental Study of a High-Efficiency Helium Twin-Screw Compressor*, Cryogenics, 116, 103286, https://doi.org/10.1016/j.cryogenics.

[8] ZHAO B., SONG H., GAO D., XU L., 2020, *Flow and Heat Transfer Coupling Analysis of Oil-Gas Two-Phase Fluid in Clearance of Single Screw Compressor Based on Fuzzy Curvelet Finite Element Method*, Case Studies in Thermal Engineering, 22, 100788, https://doi.org/10.1016/j.csite.

[9] Li Y., PEI P., MA Z., REN P., HUANG H., 2020, *Analysis of Air Compression, Progress of Compressor and Control for Optimal Energy Efficiency in Proton Exchange Membrane Fuel Cell*, Renewable and Sustainable Energy Reviews, 133, 110304, https://doi.org/10.1016/j.rser.

[10] PENG C., WU W., ZHANG Z., XIE J., FENG Q., HE Z., 2021, *Dynamic Characteristics Improvement of the Single Screw Compressor with Odd-Grooves Screw Rotor*, International Journal of Refrigeration, 132, 100–108.

[11] YANG S., OUYANG H., WU Y., WANG L., MEI L., WANG H., 2021, *CFD Simulation for the Internal Pressure Characteristics of an Oil-Injected Twin-Screw Refrigeration Compressor*, International Journal of Refrigeration, 126, 143–154.

[12] ZHANG Z., WU W., 2021, *Numerical Investigation of Thermal Deformation of Meshing Pairs in Single Screw Compressor*, *Applied Thermal Engineering*, 188, 116614, https://doi.org/10.1016/j.applthermaleng.

[13] LIU J., LI Q., WANG F., ZHOU L., 2012. *A New Model of Screw Compressor for Refrigeration System Simulation*, International Journal of Refrigeration, 35, 861–870.

[14] PARK S.-Y., HI-KOAN L., GYUN-EUI Y., SANG-DON M., 2010, *A Study on the Machining of Compressor Rotors Using Formed Tools*, International Journal of Precision Engineering and Manufacturing, 11, 195–200.

[15] WEI J., HUA Q., WANG J., JIANG Z., WANG J., YUAN L., 2020, *Overview of the Development and Application of the Twin Screw Expander*, Energies, 13, 6586, https://doi.org/10.3390/en13246586.

[16] WU Y.-R., FONG Z.-H., 2008, *Rotor Profile Design for the Twin-Screw Compressor Based on the Normal-Rack Generation Method*, Journal of Mechanical Design, 130/4, https://doi.org/10.1115/1.2839003.

[17] PARK S.-Y., HI-KOAN L., GYUN-EUI Y., SANG-DON M., 2010, *A Study on the Machining of Compressor Rotors Using Formed Tools*, Materials Science, Business, International Journal of Precision Engineering and Manufacturing, https://doi.org/10.1007/S12541-010-0022-3.

[18] CHEN C.-B., 2007, *Discussion on the Problems Related to NC Machining of Toroid-Shaped Taper Cutter with Constant Angle Between Cutting Edge and the Cutter Axis*, The International Journal of Advanced Manufacturing Technology, 35, 493–504.

[19] TEODOR V., POPA I., OANCEA N., 2010, *The Profiling of End Mill and Planing Tools to Generate Helical Surfaces Known by Sampled Points*, International Journal of Advanced Manufacturing Technology, 51/5–8, 439–452.

[20] HE X., PAN C., WU M., JI X., ZHANG R., 2015, *A Twin-Screw Rotor Profile Design and Computational Fluid Dynamic Simulation Method*, Materials Research Innovations, 19/8, 721–726.

[21] AKULINICHEV P., ZENIN I., GONCHAROV A., 2020, *Choice of Finishing and Strengthening Treatment Method for Cycloidal Screw Surfaces for Multi-Product Production Conditions*, IOP Conference Series: Materials Science and Engineering, 963, 012013.

[22] YU D.-Y., DING Z., 2020, *Geometric Characteristics Analysis and Parametric Modeling for Screw Rotor Precision Machining*, The International Journal of Advanced Manufacturing Technology, 107, 3615–3623,

[23] STOSIC N., SMITH I., KOVACEVIC A., MUJIC E., 2011, *Review of Mathematical Models in Performance Calculation of Screw Compressors*, International Journal of Fluid Machinery and Systems, 4/2, 271–288.

[24] LUCIA P., PATIC P., DUTA L., RUNCEANU A., 2010, *Modeling and Simulation of Cycloid Curves with Application in Robotics*, Revista Fiabilitate si Durabilitate, 2/6, ISSN 1844 – 640X.

[25] TIEN D.H., DUC Q.T., VAN T.N., NGUYEN N.-T., DO DUC T., DUY T.N., 2021, *Online Monitoring and Multi-Objective Optimisation of Technological Parameters in High-Speed Milling Process*, The International Journal of Advanced Manufacturing Technology, 112, 2461–2483.